EUROPEAN ORGANIZATION FOR NUCLEAR RESEARCH

CERN-LEP-VA/87-64

SUPERCONDUCTING CAVITIES PRODUCED BY MAGNETRON SPUTTERING OF NIOBIUM ON COPPER

by

C. Benvenuti, D. Bloess, E. Chiaveri, N. Hilleret, M. Minestrini, W. Weingarten

ABSTRACT

The deposition of thin niobium films on copper is an attractive solution to improve the thermal stability of superconducting rf cavities. First results obtained with a bias diode system have confirmed the interest of this approach. As an alternative to the diode configuration, a cylindrical magnetron system has been developed at CERN which combines the advantages of a simpler design and of a shorter coating duration. The coating systems and procedure are described together with the physical properties of the niobium films and the results obtained on rf cavities. Q_o values in excess of 2×10^9 at 5 MV/m have been reproducibly achieved on single cell 500 MHz cavities and a Q_o value of 6.2×10^9 was reached at 5 MV/m on a 4 cell 352 MHz cavity. Together with these excellent results, Nb coated copper cavities also present some inconveniences such as the sporadic appearance of blisters in the Nb film and a faster decrease of Q_o with increasing field. The results so far achieved are presented and discussed.

Geneva, November 1987

Paper presented at the 3rd Workshop on RF Superconductivity, Argonne National Laboratory, September 1987

1. INTRODUCTION

The energy upgrading of LEP (Large Electron Positron collider, actually being built at CERN) from 55 GeV to about 100 GeV requires the installation of 256 superconducting accelerating cavities (1). Very promising results have been obtained with bulk niobium cavities (2) but this material suffers from its relatively poor thermal conductivity resulting in thermo magnetic breakdown at high fields. In order to circumvent this weakness, elaborated methods to purify niobium have been developed leading to an increased thermal conductivity and hence stability of the cavities. Another possible approach is to deposit a thin superconducting film on to a cavity made of a material with high thermal conductivity such as copper. Since 1980 this line is pursued at CERN and good results with a diode sputtering system have been obtained (3)(4). However, the diode sputtering configuration has two basic disadvantages: a complex mechanical design due to the rotation of the cathodes and a long coating duration (24 hours for a 1 μm layer). To improve on these two points a different coating facility has been developed, based on a magnetron sputtering system (5). The new coating facility and the main results obtained will be described in this paper.

2. DESIGN OF THE COATING FACILITY

2.1 Principle of magnetron discharge

Among the various methods usually gathered under the heading of physical vapour deposition, sputtering has specific advantages for the deposition of high quality refractory metals (6). This method involves the creation of a self-sustained glow discharge and its simplest version is the diode configuration. In this configuration, the discharge is sustained thanks to the ionization of the residual gas by electrons emitted from the cathode under the impact of ions and/or created in ionizing collisions. Larger deposition rate at lower pressure can be obtained by increasing the number of collisions between the electrons and the gas before the electrons are lost. This is achieved in magnetron type discharges (7) by superposing to the electrical field, perpendicular to the cathode, a magnetic field which

traps the electrons on close trajectories. In cylindrical structures the magnetic field is parallel to the cathode surface. (cylindrical magnetron configuration (8)). Because of the axial symmetry of the rf cavities, this configuration was adopted for the various coating systems.

A schematic view of the coating system for 500 MHz cavities is given in figure 1. The cathode consists of a vacuum tight stainless steel tube (100 mm diameter) surrounded by a niobium liner. A solenoid providing the required magnetic field (about 1.4×10^{-2} T at 60 mm from the central axis) is contained inside the stainless steel tube. Liquid freon circulating inside this tube cools the cathode and the magnet. A ceramic piece insulates electrically the inner tube from the copper cavity held at ground potential. The niobium liner is made in several parts. The central zone, sputtered during the coating of the cavity, is made of high purity niobium (residual resistance ratio RRR =100). For the cut-off tubes, reactor grade niobium (RRR=40) is used.

The 352 MHz single cell cavities are coated by means of this same system. However, the discharge current is increased to maintain the same niobium deposition rate. In the case of the 352 MHz 4-cells cavities (4C), another system (figure 2) was constructed, based on an extrapolation of the 500 MHz set up. The central stainless steel tube has in this case an outer diameter of 133 mm. As for the 500 MHz cavities, the parts of the Nb liner corresponding to the centre of each cell are made out of high purity niobium (RRR=100).

For the coating of the coupling tubes not shown in Fig. 2, having a diameter of 100 mm and a length of 230 mm, small bias diodes have been developed. They allow the coating of these tubes in one hour and operate at a voltage of 1500 V and at a pressure of 4×10^{-2} Torr. A magnetron cathode is under study also for this application.

2.2 The vacuum systems

Both deposition systems are pumped by turbomolecular pumps (pumping speed respectively 270 l/s for the monocell system and 400 l/s for the 4C system). Prior to the deposition, the systems are

baked at 150°C during 24 hours. After such a bakeout, a pressure in the low 10^{-9}/high 10^{-10} Torr range is obtained.The high purity argon gas (less than one ppm total impurity concentration) required for the sputtering is introduced by a baked injection line. Its purity is checked prior to deposition using the residual gas analyser. During the discharge the main impurity is hydrogen (less than 1%, depending on the position of the discharge with respect to the gas analyser).

3. PREPARATION OF THE CAVITIES AND COATING PROCEDURE

The copper cavities are manufactured in a similar way to bulk niobium cavities (9). Half cells are spun and electron beam welded using an internal gun. After the welding, the cavities are degreased and etched in order to remove the surface damaged layer (about 80 μm) using a chemical bath (10). A second chemical treatment (10), carried out using a similar bath produces a polished copper surface (roughness R_A~0.1 μm) presenting the following surface composition determined by Auger spectroscopy: Cu 41%, C 36%, O 10%, Cl 8%, N 4%, S 1%. The oxide layer present at the surface is approximately 1 nm thick. After chemical polish, the cavity is thoroughly rinsed with high purity dust free demineralized water (resistivity 18 M Ω.cm) then with dust free ethanol. The cathode is inserted in the cavity in front of a laminar flow wall, the cavity is installed on the coating system and baked during 24 hours at 150°C. The coating of the cavity is carried out in several steps using optimized parameters (5). The sequence for a 4C cavity is typically the following:

1) Pre-sputtering in the upper and lower transition pieces ($6x10^{-4}$ Torr, 700 V, 2 A, 4 mn);

2) Coating of the upper and lower cut-off tubes ($6x10^{-4}$ Torr, 400 V, 3 A, 36 mn). During this operation the magnet is displaced continuously over the cut-off length;

3) Coating of the cells ($6x10^{-4}$ Torr, 400 V, 15.6 A, 50 mn for the outer cells, 75 mn for the inner cells), with magnet positioned in the centre of the cell.

Several coatings are done on the same cavity. After each deposition, the niobium film is dissolved, the cavity is tumbled several days with alumina chips and then repolished according to the precedent recipe. For 352 MHz 4C cavities, the tumbling is replaced by an etching (80 μm removed) as described above.

4. PHYSICAL PROPERTIES OF THE NIOBIUM FILM

4.1 Thickness profile

The coating thickness changes along a meridian of the cavity due to the variation both of the distance between the cathode and the cell and of the angle between the normal to the cathode and a point of the cell. However, it is constant in a plan perpendicular to the cavity axis because of the axial symmetry of the system. Thickness profiles have been obtained by measuring with a scanning electron microscope samples cut from strips placed in test cavities or cut from a cavity in the case of 4C cavities. Inside 500 MHz cavities, the thickness varies from 1.2 μm at the equator to 1.7 μm at the iris. In the case of 352 MHz 4C cavities, a minimum thickness (0.7 μm) is measured at the irises, while the thickness in the cells varies between 1.5 μm and 2 μm.

4.2 Measurements of Tc and RRR

The critical temperature (Tc) and the RRR have been measured on samples mounted at various places in test cavities or cut from a 4C cavity. The results obtained on both cavity types are similar. In the case of a 4C cavity, coated according to the conditions given in chapter 3, the results are shown on figure 3 where two sets of measurements are given. The first give the Tc measured inductively (Tc_I) on samples cut from a 4C copper cavity. The second presents results (Tc_R and RRR) measured resistively on quartz samples coated according to the standard procedure in a 4C steel cavity, identical in shape to the 4C copper cavity. The general trend is a higher Tc and RRR value in the cells and a minimum Tc in the lower cut-off. Furthermore the lower cell (closer to the pump) has systematically a lower Tc and RRR than the other cells.

4.3 Chemical composition of the films

The mean impurity content in the films was measured using various methods: nuclear reactions for carbon and oxygen, elastic recoil diffusion analysis (ERDA) for hydrogen. Mean concentrations of metallic impurities (Fe and Cu) were obtained by atomic absorption from the film after having disolved the copper substrate. The results obtained by the differents methods are summarized in Table 1:

TABLE 1

Impurities' content in the Nb films

Element	Content at.%
H	1
C	0.4
O	1.6
Cu	0.06
Fe	0.005
N	not measured

Neither X ray dispersive analysis, nor Auger spectroscopy revealed any trace of argon in the film i.e. the argon concentration is lower than 1%. Surface composition and concentration profiles were also obtained by Auger spectroscopy and secondary ion emission (SIMS). The Auger spectra shown on figure (4) give the concentration of impurities present at the surface of a sample: the usual contamination for an air exposed niobium sample is visible (56 at.% C, 27 at.% O, 17 at.% Nb). After a short erosion (27 nm), these impurities become undetectable in the Auger spectrum. On figure 5 SIMS profiles of various impurities (H, C, N, O, Cu) are displayed for a 800 nm thick layer obtained under the standard conditions. Outside the first 50 nm and copper excepted, the concentration of impurities in the film is relatively constant. In the case of copper there is a deep minimum ($1x10^{17}$ at.cm^{-3} between 100 and 400 nm) and a large interdiffusion zone of copper in the niobium layer between 500 nm and 800 nm. Oxygen and nitrogen have comparable concentration, close to 1%, carbon and hydrogen are present at lower

content: about 0.5 at.% in the layer. Integration of these profiles gives values in good agreement with the above quoted mean concentrations.

As impurities can greatly affect the superconducting properties of niobium (17), it is important to understand their origin. When assuming that impurities are introduced during the film growth and taking into account the deposition rate of niobium (2.2×10^{15} at.cm^{-2} s^{-1}, i.e. 0.5 nm s^{-1}), these concentrations would represent a flow of 5×10^{-3} Tl s^{-1} for O_2 and 1.7×10^{-3} Tl s^{-1} for H_2. Such a high gas flow would have been easily detected during the routine checking of the gas purity prior to the coating (cf. paragraph 2.2), hence the impurities detected in the film are not introduced with argon in the vacuum system.

Moreover, the amount of impurity present at the copper surface is also too small by several orders of magnitude to be responsible for the impurity content in the film.

These observations exclude that most of the impurity content stems from the coating stage. On the other hand, it has been shown (11)(12) that, depending on the structure of the film, impurity incorporation can take place when exposing the film to air. This possibility is supported by the large film content of N_2,a gas not detected in the gas phase during the coating. On the other hand, copper detected at the surface of the film indicates the presence of porosities which may result in O_2 and N_2 absorption when the coated cavity is exposed to air.

5. RESULTS

The variation of the deposition parameters has been carried out on 500 MHz cavities on which most of the work has been concentrated up to now. The optimised deposition conditions were then extrapolated to 352 MHz single cell cavities, later on to 352 MHz 4C cavities.

5.1 500 MHz single cell cavities

Twenty-five coatings have been carried out on 500 MHz cavities using the magnetron system. Part of this work aimed at testing various cleaning procedures and will not be considered in this paper. The results given hereafter refer to cavities chemically prepared in the same standard way and hence they are specifically representative of the coating method performance. Figure 6 shows the variation of Q with the accelerating field at 4.2 K for 4 cavities coated with a cathode voltage of 700 V and a discharge power of 3 kW, giving on samples RRR=8; figure 7 gives the results obtained on another set of 4 cavities coated with different deposition parameters (400 V, 3 kW, giving on samples RRR=14). The results obtained are summarised in Table 2. The following characteristic features may be deduced from these results:

TABLE 2

Deposition conditions	$Q_o(E=0)$ $\times 10^9$		$Q_o(E=5$ MV/m) $\times 10^9$	
	MAX	MIN	MAX	MIN
700 V/3 kW	4.8	3.8	2	1.5
400 V/3 kW	6	4.8	3.5	2.1

- Good reproducibility of cavity performance for the same coating procedure
- High Q_o at low field, higher for the cavities obtained at 400 V, 3 kW i.e. for films with a higher RRR
- An exponential decrease of Q with increasing the accelerating field
- On some curves a sudden drop of Q at a given field level

This last feature (Q switch) can be traced using the temperature mapping system and is due to small niobium regions (usually between 1 and 0.1 mm^2) in bad thermal contact with the copper ('blisters'). These defects are sporadic in nature and are consequent to a lack of

adhesion between niobium and copper due to the presence on the copper surface of foreign particles or rinsing residues. Most of the small blisters do not contribute significantly to the surface resistance at 5 MV/m, because of the preponderant effect of the field dependent losses, as shown by figure 8.

The curves $Q_o(Ea)$ can be represented (13) by an equation of the type $Q_o(Ea)=Q_o(0).\exp(-\alpha.Ea)$ where $Q_o(Ea)$ and $Q_o(0)$ are respectively the quality factor of the cavity at Ea and at very small accelerating field. The values of $Q_o(0)$ and α can be derived from the $Q_o(Ea)$ curves. The field dependent surface resistance can be approximated by $\alpha G/Q_o(0)$ (13).

Another peculiarity of the niobium coated copper cavities is that $Q_o(Ea)$ is independent of static magnetic field (13). For bulk niobium cavities the quality factor is decreased by 'frozen in' magnetic flux when they are cooled in presence of an external magnetic field. This phenomenon was not observed with niobium coated cavities and it was also shown that a low external static magnetic field does not affect the slope of the Q(Ea) curves (13).

Sputtered cavities exhibit also a low residual resistance (see figure 9). The residual resistance is not influenced by the deposition parameters, i.e. it is not directly related to the RRR of the layer. As far as field emission is concerned, the performance of sputtered cavities are comparable to those of bulk niobium and in several occasions fields as high as 8 MV/m have been reached within 10 minutes after the start of the measurements.

Last but not least, thermal quenches have never been observed and at the time of the measurements the accelerating field achievable in all cavities was always limited by the available rf power.

5.1.1 Changes in the $Q_o(Ea)$ curves after exposure to air

Two cavities were remeasured after several months exposure to laboratory air. In one case the cavity (cavity I) had been coated with 700 V cathode voltage. After an exposure of 2 months

at laboratory air, no significant changes were visible on the $Q_o(Ea)$ curves (figure 10). In the other case (cavity II, coated with 400 V cathode voltage, see figure 11) a clear degradation of $Q_o(0)$ as well as a steeper decrease of $Q_o(Ea)$ with increasing accelerating field can be observed after 9 months of exposure to laboratory air. The variation of $Q_o(0)$ and of the field dependent surface resistance, $\alpha G/Q_o(0)$, with the air exposure are given in table 3 for these two cavities.

TABLE 3

Deposition Parameters	Initial		2 Months Air		9 Months Air		After baking	
	$Q_o(0)$ $x10^9$	$\alpha G/Q_o(0)$ $x10^{-9}$	$Q_o(0)$ $x10^9$	$\alpha G/Q_o(0)$ $x10^{-9}$	$Q_o(0)$ $x10^9$	$\alpha G/Q_o(0)$ $x10^{-9}$	Q_o $x10^9$	$\alpha G/Q_o(0)$ $x10^{-9}$
700 V	3.8	7.8	4.3	11				
400 V	6.3	4.3			5	6.5	3.7	9.5

The larger observable deterioration on cavity II may be due to the longer air exposure and to its higher $Q_o(0)$ value.

5.2 352 MHz single cell cavities

Two types of such cavities were used one without coupling ports and a second one with coupling ports. The curve $Q_o(Ea)$ for the first type of cavity is given on figure 12 together with the curve measured for a bulk niobium cavity of identical shape. For the cavity without coupling port, 15 hours helium processing were necessary in order to push the accelerating field above 5MV/m. The Q_o value at 5 MV/m was $2.9x10^9$ after processing. Both the $Q_o(0)$ and the factor $\alpha G/Q_o(0)$ describing the field dependent losses are comparable to those measured on 500 MHz single cell cavities. For the cavity equipped with coupling ports a strong multipacting was experienced at the junction of the coupling ports with the cut off tube. Further experiments on this type of cavity are in progress.

5.3 352 MHz 4 cells cavities

Several attempts have been made to coat a 4C cavity with magnetron sputtering (400 V, 3 kW). Fields up to 5 MV/m were reached without thermal breakdowns but the Q values were limited by cracks located in the equatorial welds. In another case, a large defect could be related to the inadequate cleaning of the copper surface. Recently a more successful attempt was made, giving the $Q_o(Ea)$ curve shown on figure 13. The $Q_o(0)$ obtained was larger than 10^{10} and at 5 MV/m accelerating field the measured Q_o was 6.2×10^9 (more than twice the LEP design value) after 32 hours helium processing. The residual surface resistance was lower or equal to 2.8 nΩ.

6. CONCLUSIONS

A cylindrical magnetron coating system has been developed at CERN for the production of Nb coated copper superconducting cavities. This sputtering configuration offers a simple design, an improved performance of the cavities and a shorter coating time with respect to the diode configuration previously used.

Several coating conditions have been studied, resulting in the reproducible obtention of Q_o values higher than 2×10^9 for 5 MV/m accelerating field in 500 MHz cavities, for which fields up to 10 MV/m have been reached with a Q_o value exceeding 1×10^9. In a 4 cell 352 MHz cavity, a Q_o value of about 6×10^9 at 5 MV/m has been reached together with a $Q_o(0)$ of about 10^{10}.

In some cases, due to foreign particles or chemical residues, blisters may be produced in the Nb film, resulting in 'Q switches'. They can be eliminated by careful rinsing and dust-free manipulation of the copper cavity prior to the deposit.

The improved thermal stability of the coated copper cavities has also been confirmed, since the maximum achievable field in all the cavities tested was always limited by the available rf power.

Finally, the high deposition rate of cylindrical magnetron sputtering makes this configuration very attractive for the obtention of coatings of Nb based compounds of higher Tc.

Compared to bulk niobium cavities, sputtered cavities have some peculiarities (insensitivity to the presence of an external static magnetic field during cavity cooldown and stronger decrease of Q with increasing accelerating field) which have been linked to weak superconducting spots and pinholes filled with Nb_2O_5 (13). Experimental evidence exists that the variation of the deposition parameters (e.g. changing the cathode voltage from 700 V to 400 V) results in a variation of the RRR of the deposit without altering significantly the impurity content in the layer. From this observation we infer that the major part of the impurities do not play a limiting role for RRR nor for the performance of a coated cavity. On the other hand, the degradation of the performance of the cavity stored in air during 9 months and its further degradation after baking under vacuum may only be attributed in our opinion to an increase of the impurity concentration and/or a migration of a part of the impurities to a state where they degrade the quality of the cavity. The role and origin of the impurities in the deposited Nb films will be a matter of further studies. Nevertheless, the RRR of the Nb films as well as their superconducting properties can be affected also by parameters like grain size (14), lattice parameters (15), which are not directly linked to the impurity content.

REFERENCES

1. P. Bernard, H. Lengeler, E. Picasso Workshop LEP 200, Aachen Germany (September 1986).

2. P. Bernard et al., CERN-EF/RF 85-6 (1985).

3. C. Benvenuti, N. Circelli, M. Hauer, Appl. Phys. Lett. 45, 5, 583 (1984).

4. C. Benvenuti, N. Circelli, M. Hauer, W. Weingarten, IEEE-MAG, 21, 153 (1985).

5. C. Benvenuti et al., to be published.

6. D.W. Hoffman, C. Peters, Proceedings IX Int. Vac. Congress, 415, Madrid (1983).

7. J.A. Thornton, A.S. Penfold, Thin Film Processes, J.L. Vossen and W. Kern,Academic Press, New York (1978).

8. J.A. Thornton, J. Vac. Sci. Technol., 15, 2, 171 (1978).

9. E. Chiaveri, D. Lacarrere, B. Thizy, submitted to the 4th Int. Coll. on welding and melting by electron and laser beam, Cannes, (September 1988).

10. J.D. Adam, J.P. Birabeau, J. Guerin, S. Pousse, Note technique 85/SB/AC/B/3199/gp (1985).

11. W.D. Westwood, Progress in Surf. Sci. 7, 71 (1976).

12. D.W. Hoffman, Thin Solid Films, 107, 353 (1983).

13. G.Arnolds-Mayer, W. Weingarten, Applied Superconductivity Conf., Baltimore (September 1986).

14. E.I. Alessandrini, R.B. Laibowitz, J.M. Viggiano, J. Vac. Sci. Technol. 18, 2, 318 (1983).

15. G. Heim, E. Kay, J. Appl. Phys., 46, 9, 4006 (1975).

16. W. De Sorbo, Phys. Rev. 132, 1, 107 (1963).

17. C.C. Koch, J.O. Scarbrough, D.M. Kroeger, Phys. Rev. B, 9, 3, 888 (1974).

FIGURE CAPTIONS

Figure 1 : The coating system for 500 MHz cavities.

Figure 2 : The coating system for 4-cell 352 MHz cavities.

Figure 3 : Critical temperatures T_{CR} and T_{CI} and resistivity ratio RRR as a function of the position in a 4 cell 352 MHz cavity.

Figure 4 : Auger spectrum of the surface and after a 27 nm erosion of a sputtered niobium layer.

Figure 5 : SIMS profiles of the impurity content in a 800 nm niobium layer.

Figure 6 : Curves $Q_o(Ea)$ for 500 MHz cavities coated with 700 V sputtering voltage.

Figure 7 : Curves $Q_o(Ea)$ for 500 MHz cavities coated with 400 V sputtering voltage.

Figure 8 : Various contributions to the surface resistance at 5 MV/m for 3 different 500 MHz cavities.

Figure 9 : Histogram of the residual resistance for the 500 MHz cavities.

Figure 10 : $Q_o(Ea)$ curves for a 500 MHz cavity

A : 1 week after the deposition
B : after two months' storage in laboratory air.

Figure 11 : $Q_o(Ea)$ curves for a 500 MHz cavity

A : 1 week after the deposition
B : after nine months' storage in laboratory air
C : after a bakeout at 150°C subsequent to B.

Figure 12 : $Q_o(Ea)$ curve for a 352 MHz single cell cavity.

Figure 13 : $Q_o(Ea)$ curve for a 352 MHz 4-cell cavity.

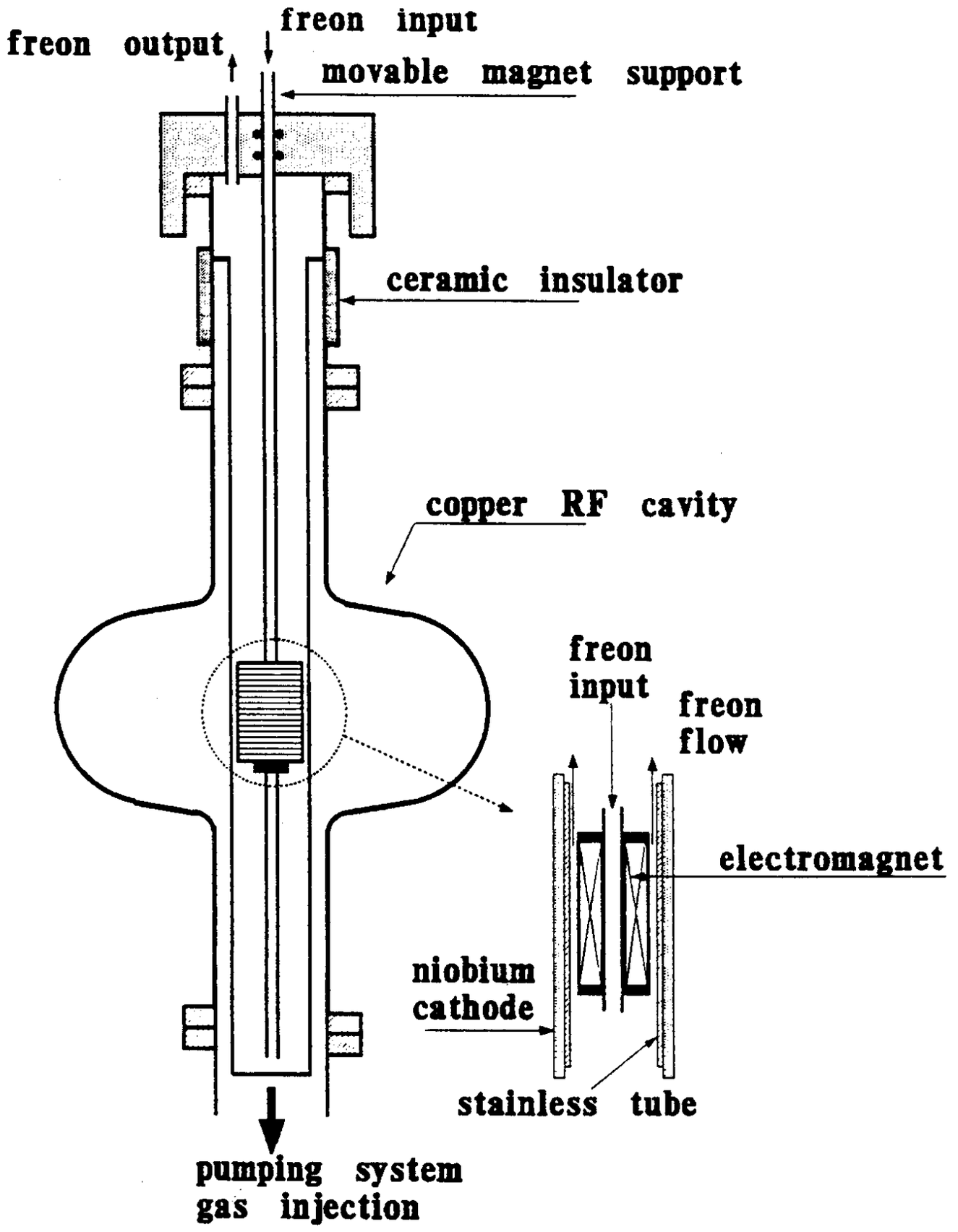

SCHEMATIC ASSEMBLY OF THE MAGNETRON SPUTTERING CONFIGURATION

Figure 1

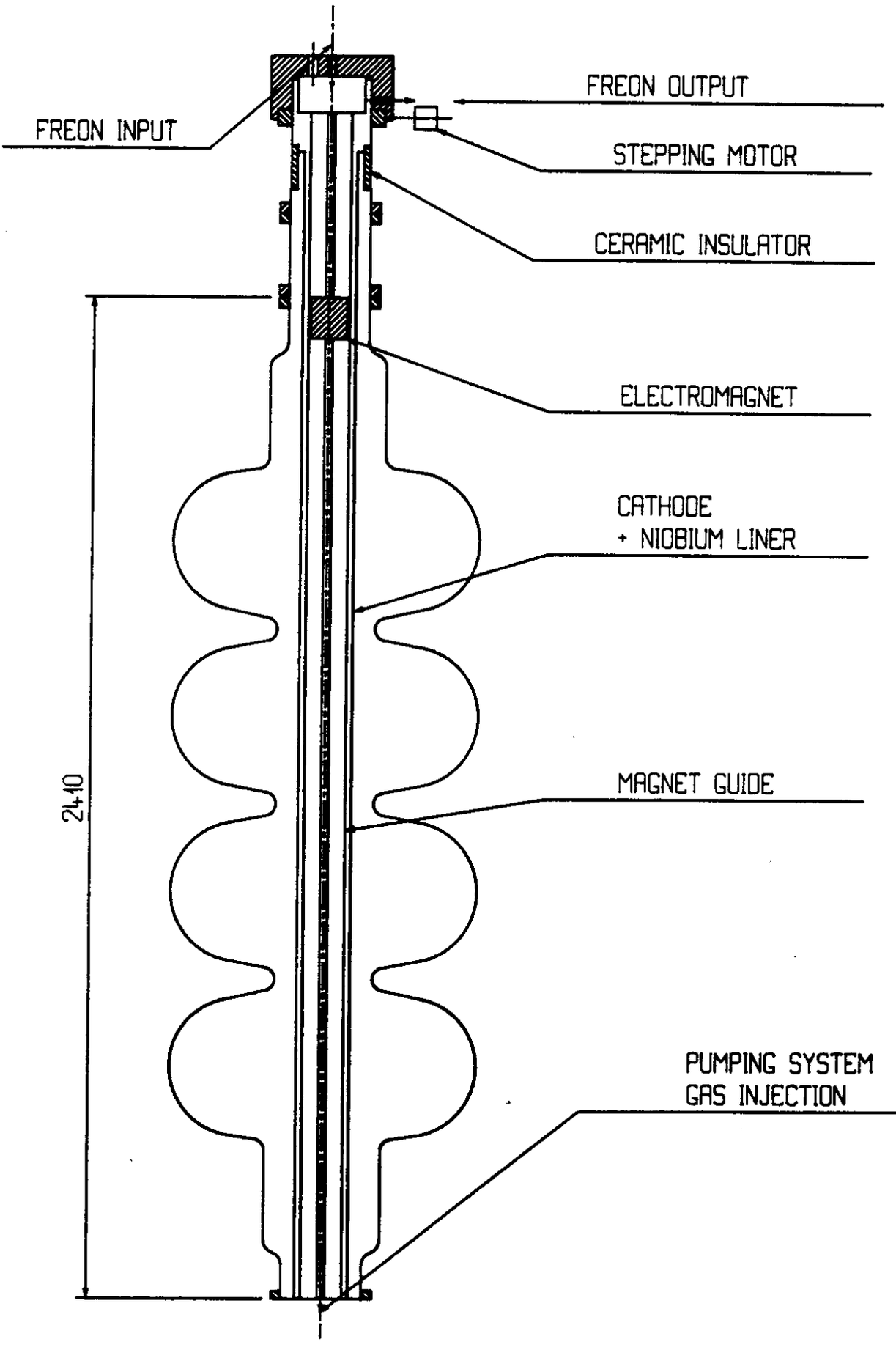
FREON OUTPUT
FREON INPUT
STEPPING MOTOR
CERAMIC INSULATOR
ELECTROMAGNET
CATHODE
+ NIOBIUM LINER
2410
MAGNET GUIDE
PUMPING SYSTEM
GAS INJECTION

Figure 2

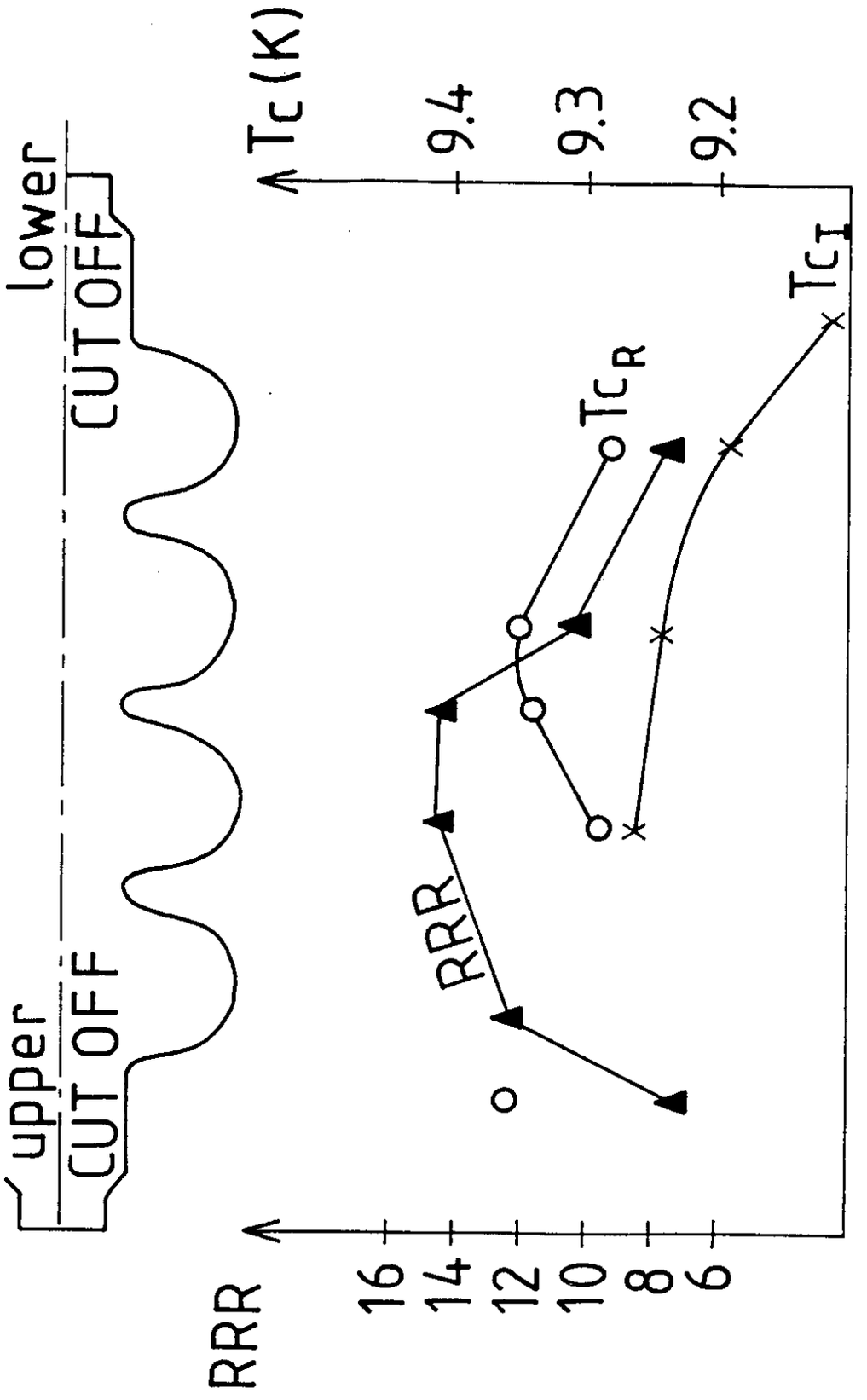
upper
CUT OFF
lower
CUT OFF
RRR
16
14
12
10
8
6
Tc (K)
9.4
9.3
9.2
RRR
TcR
TcI

Figure 3

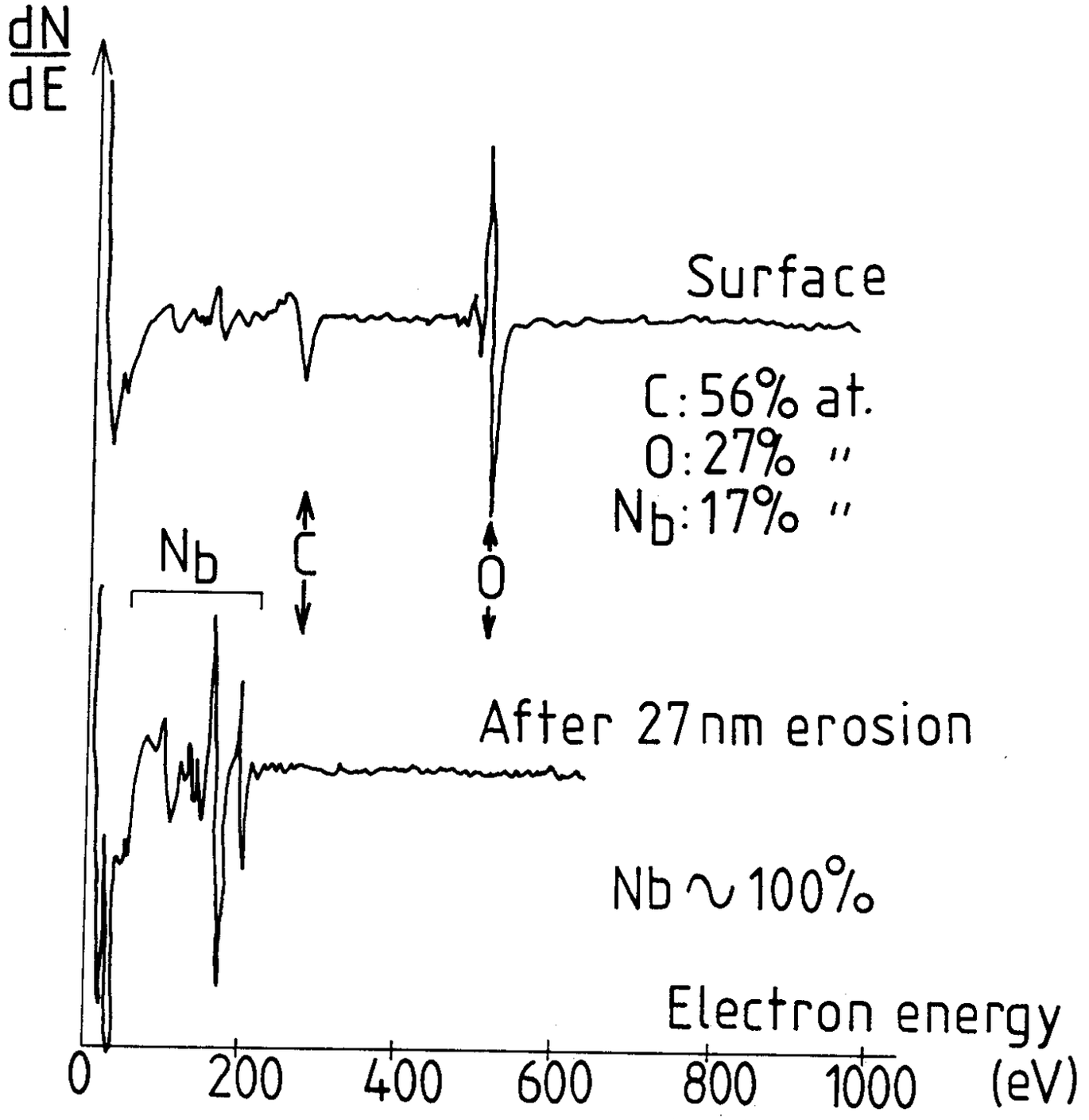
dN/dE
Surface
C: 56% at.
O: 27% "
Nb: 17% "
Nb
C
O
After 27 nm erosion
Nb ∼ 100%
Electron energy
0
200
400
600
800
1000
(eV)

Figure 4

Figure 5

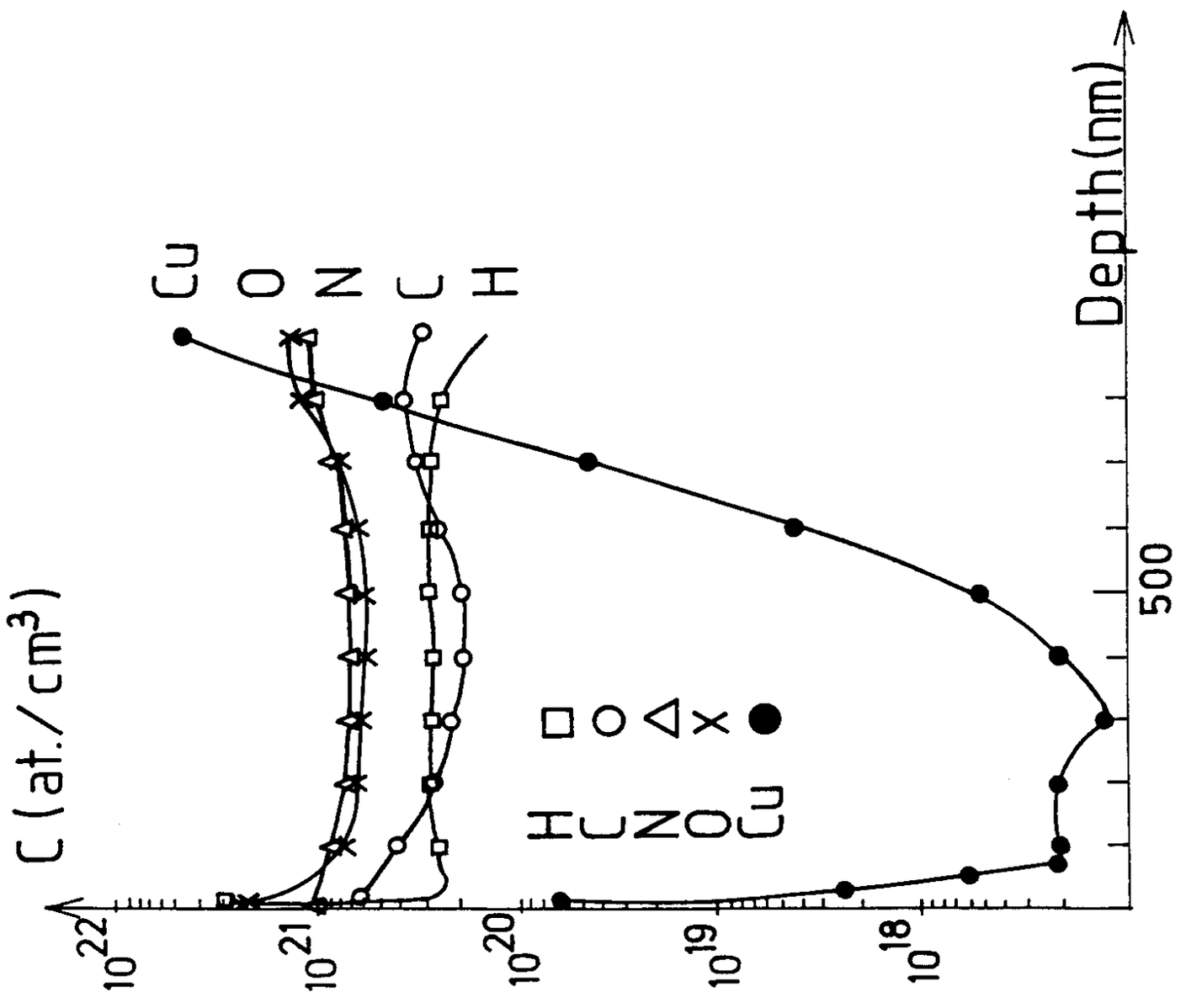

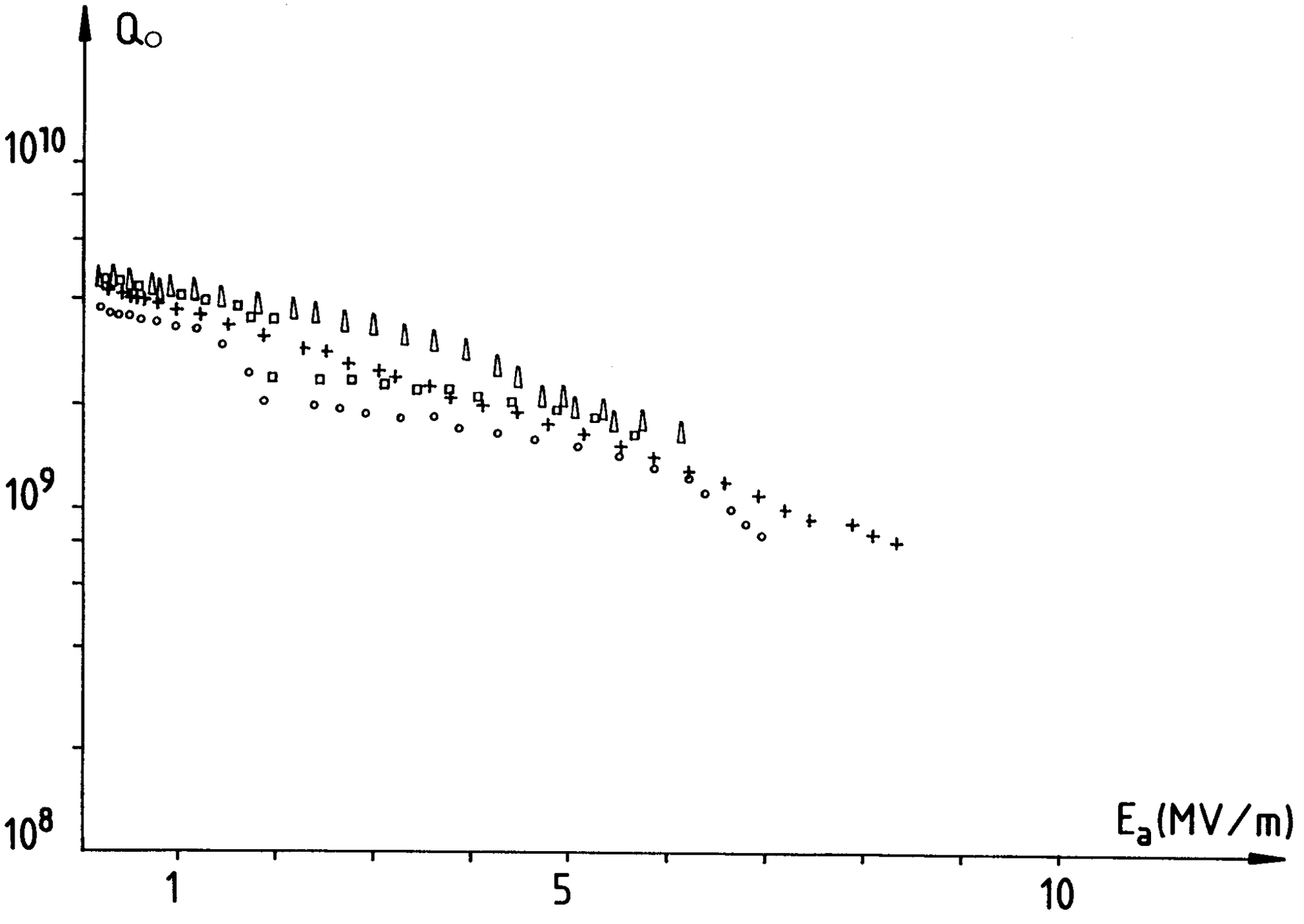

Figure 6

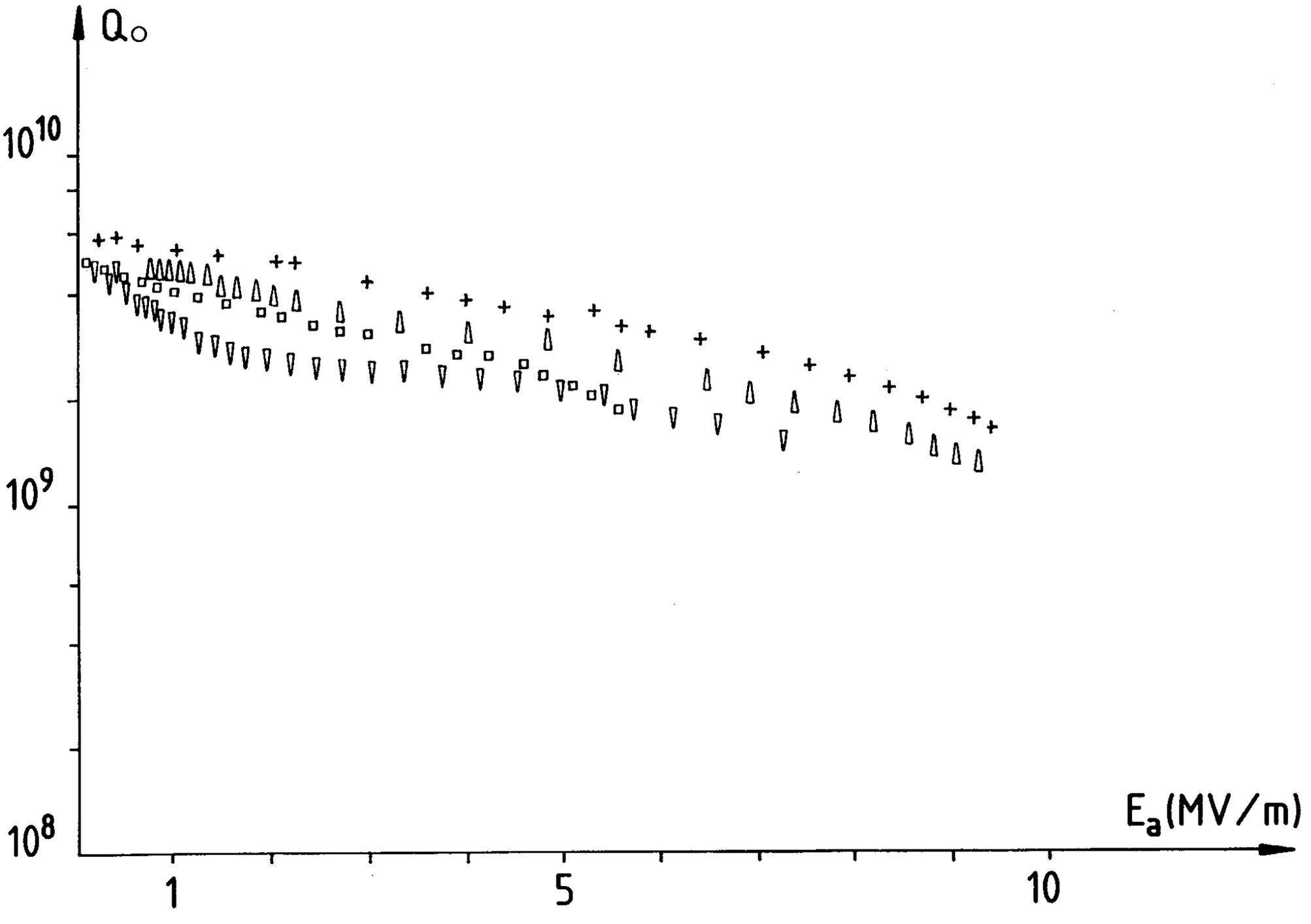

Figure 7

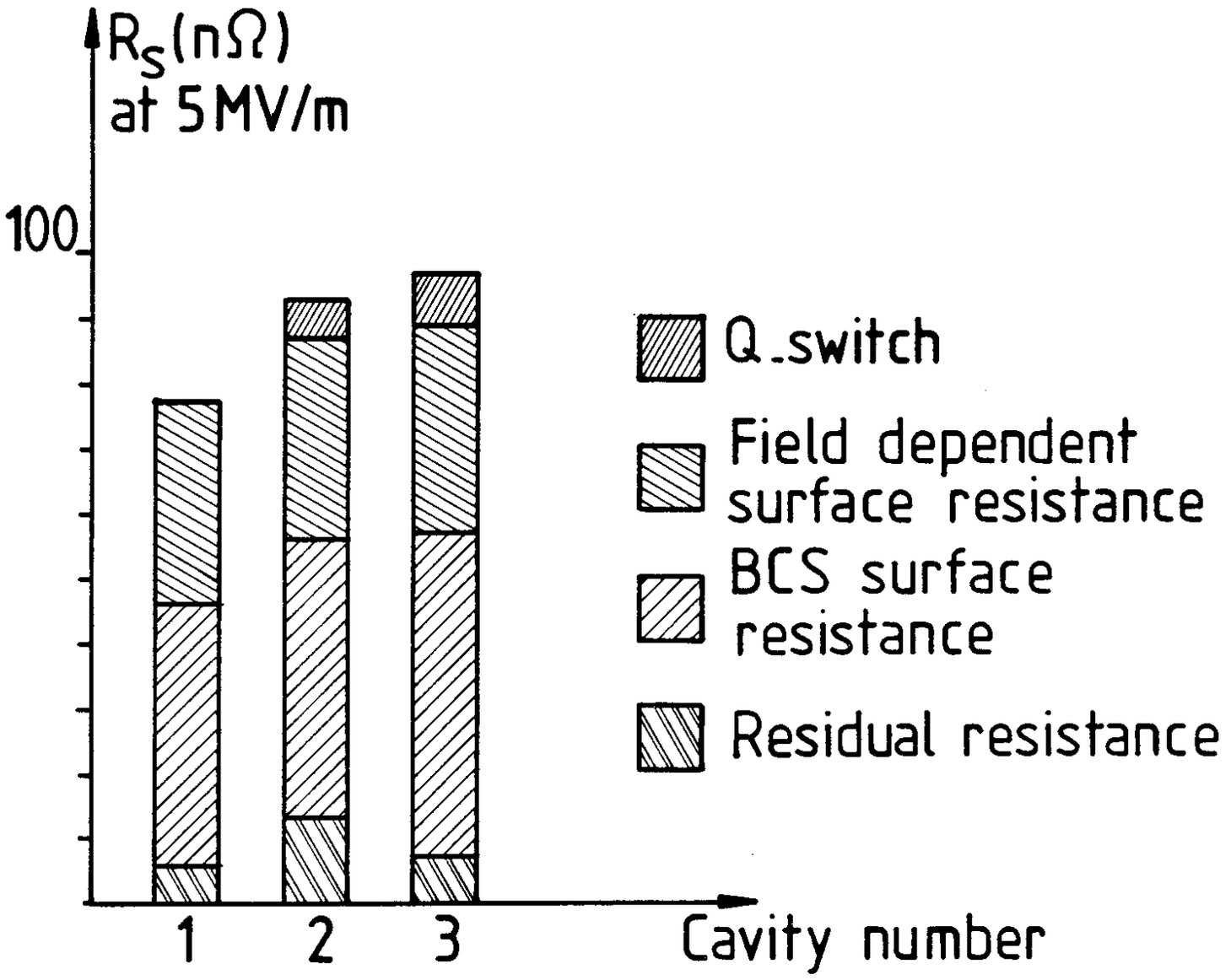
R_s(nΩ)
at 5MV/m
100
Q-switch
Field dependent surface resistance
BCS surface resistance
Residual resistance
1
2
3
Cavity number

Figure 8

Figure 9

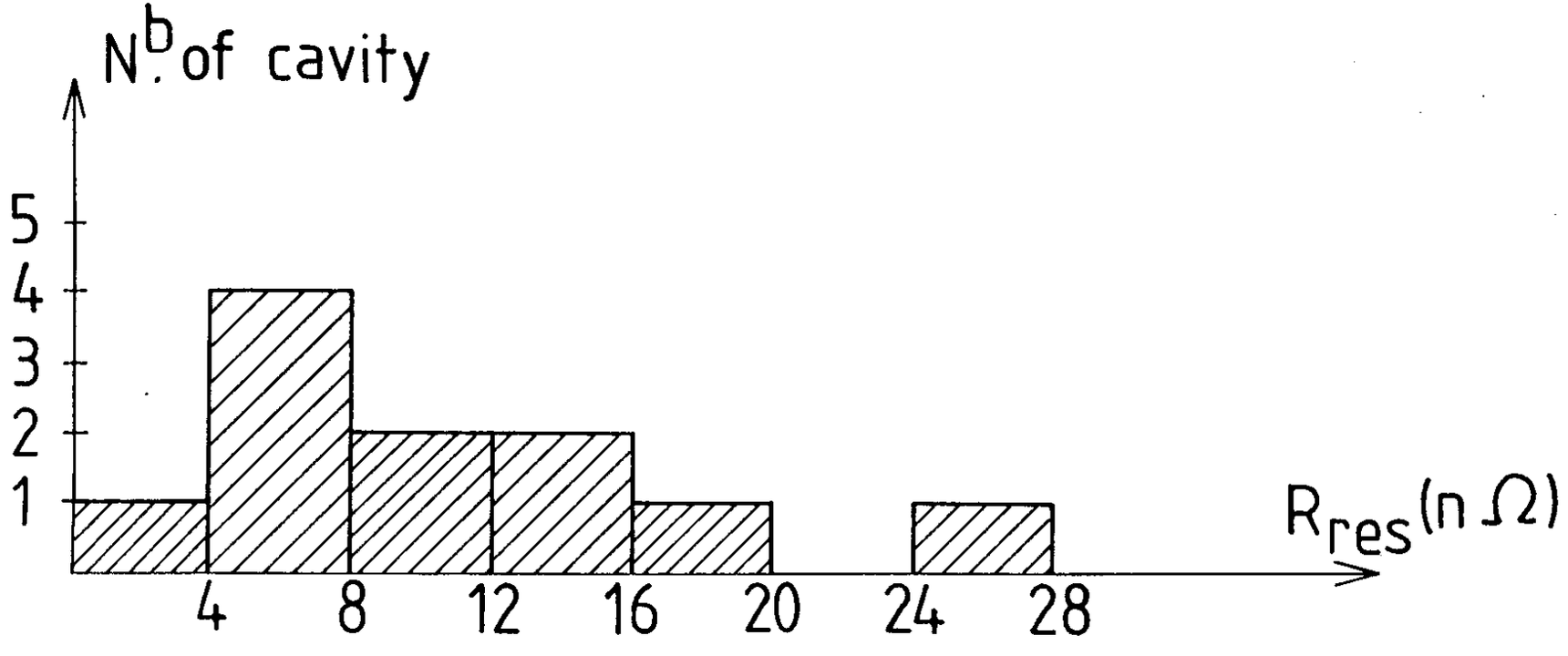

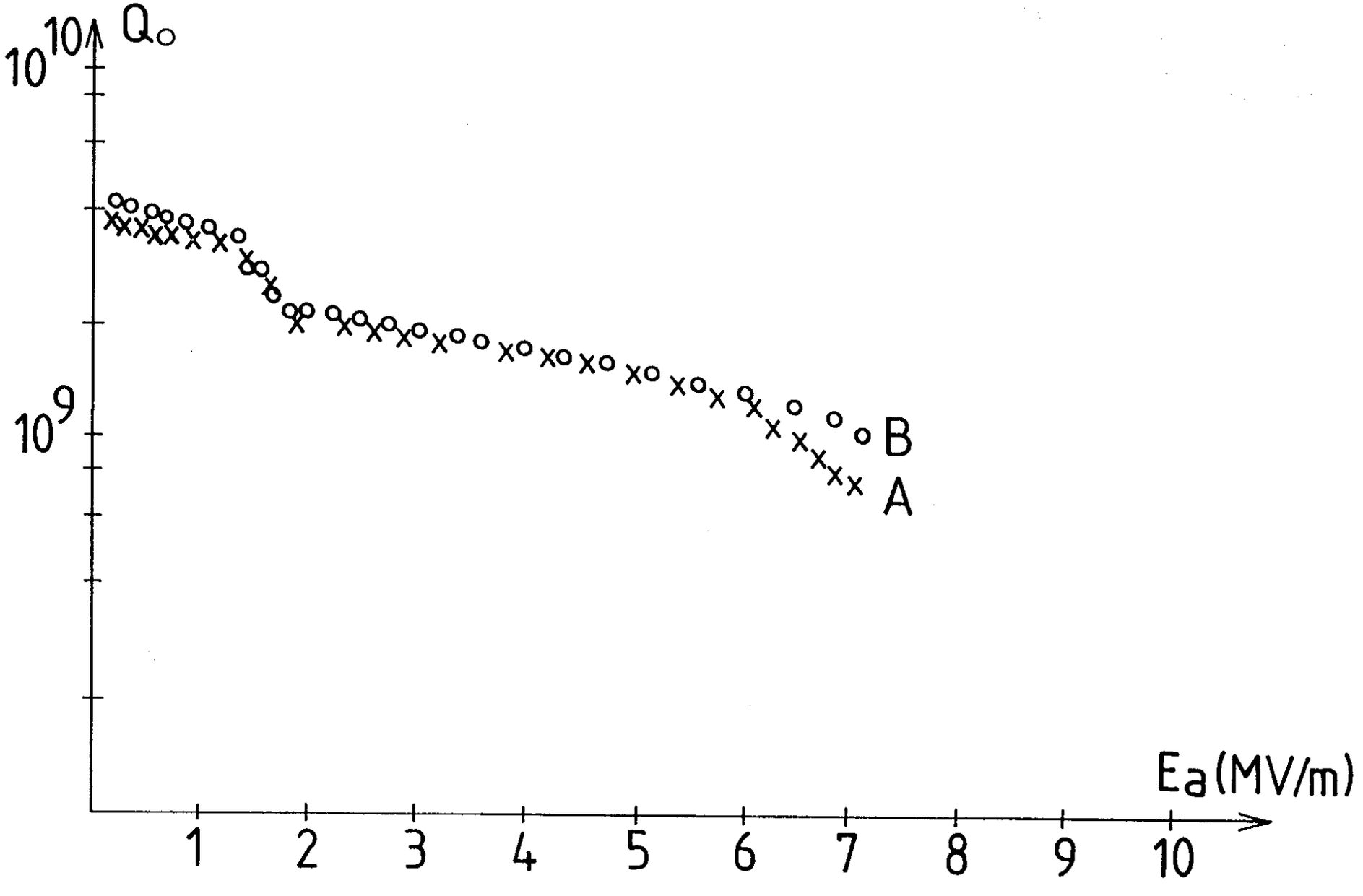

Figure 10

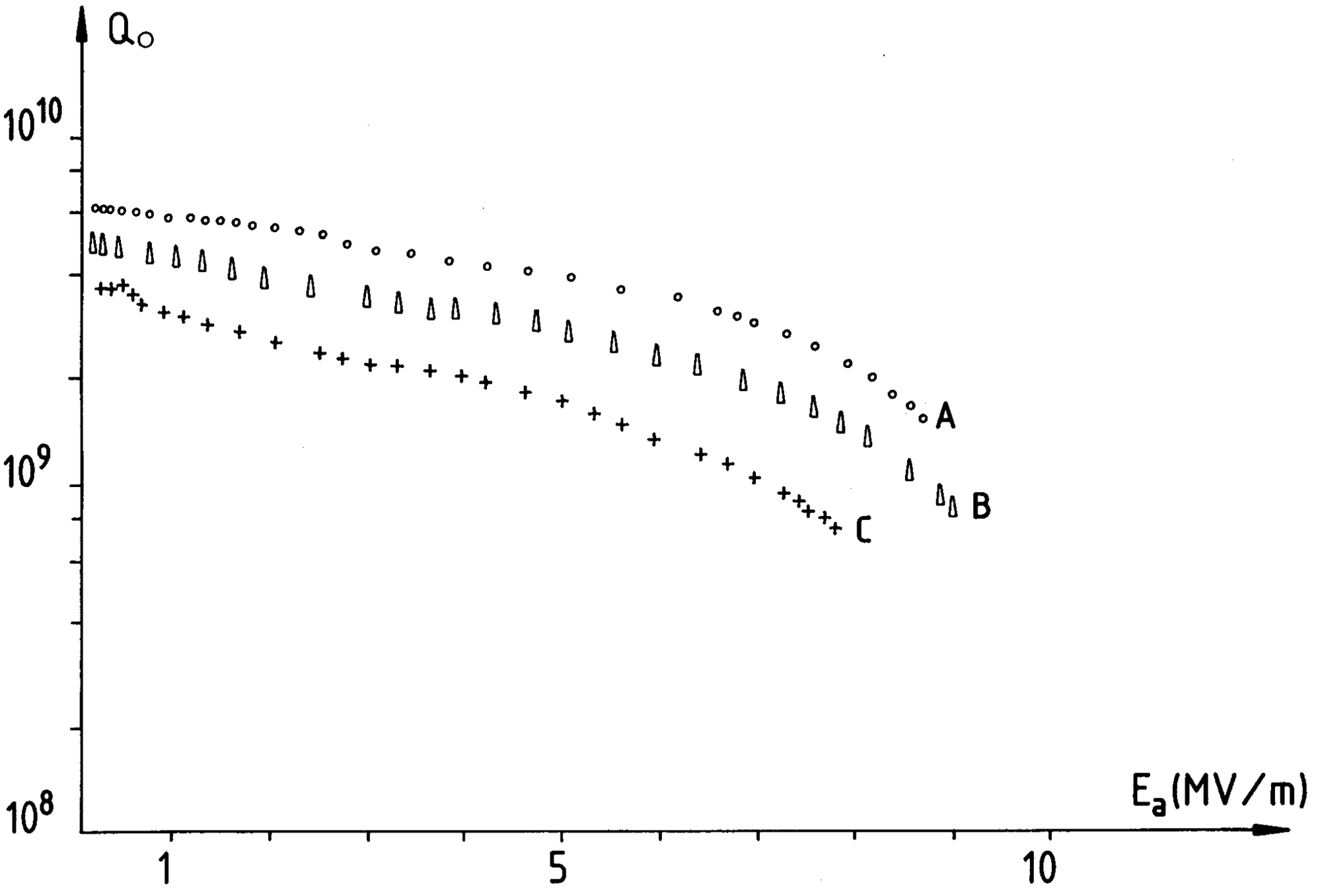

Figure 11

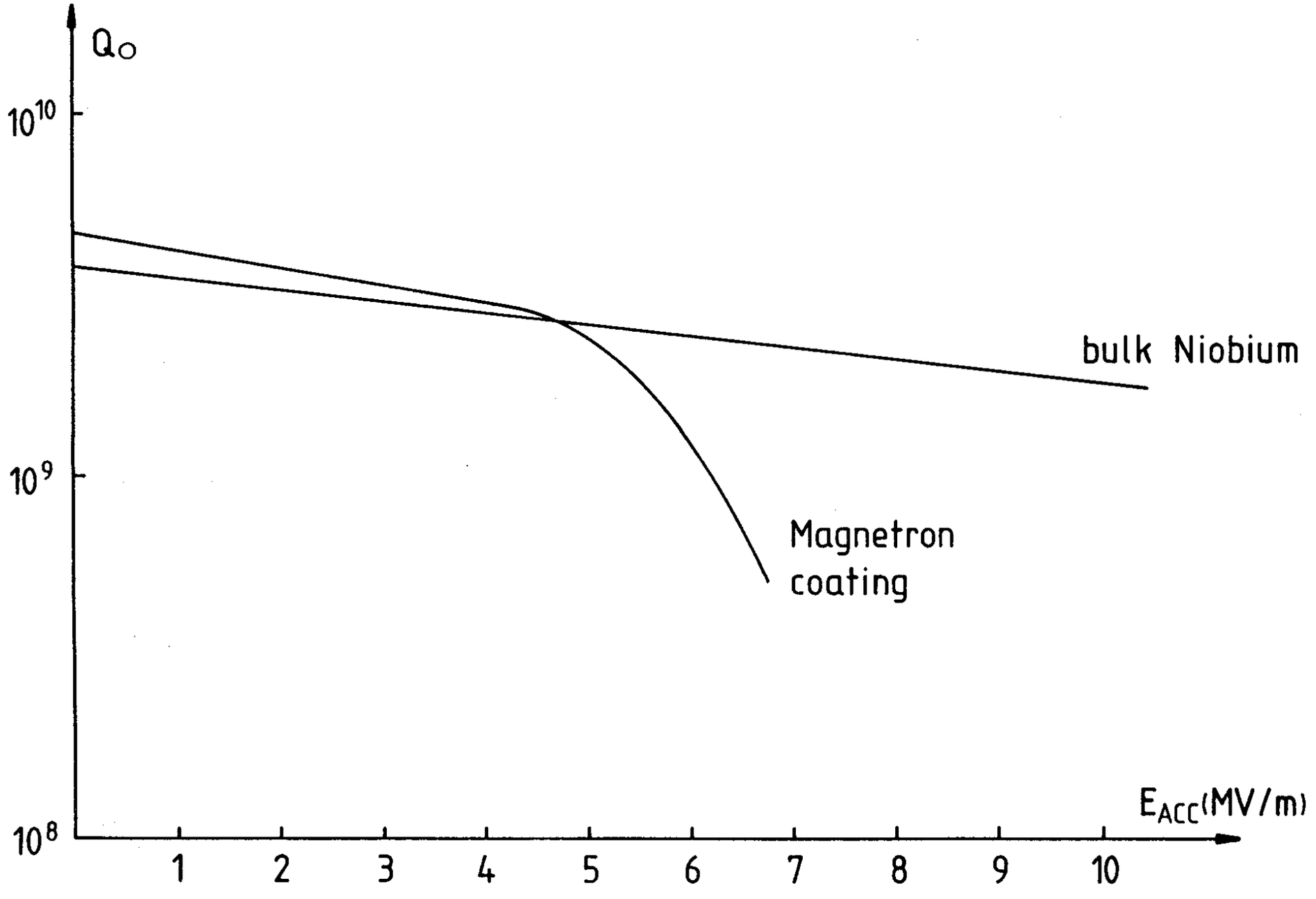
Q_O
10^{10}
10^9
10^8
bulk Niobium
Magnetron
coating
E_{ACC}(MV/m)
1
2
3
4
5
6
7
8
9
10

Figure 12

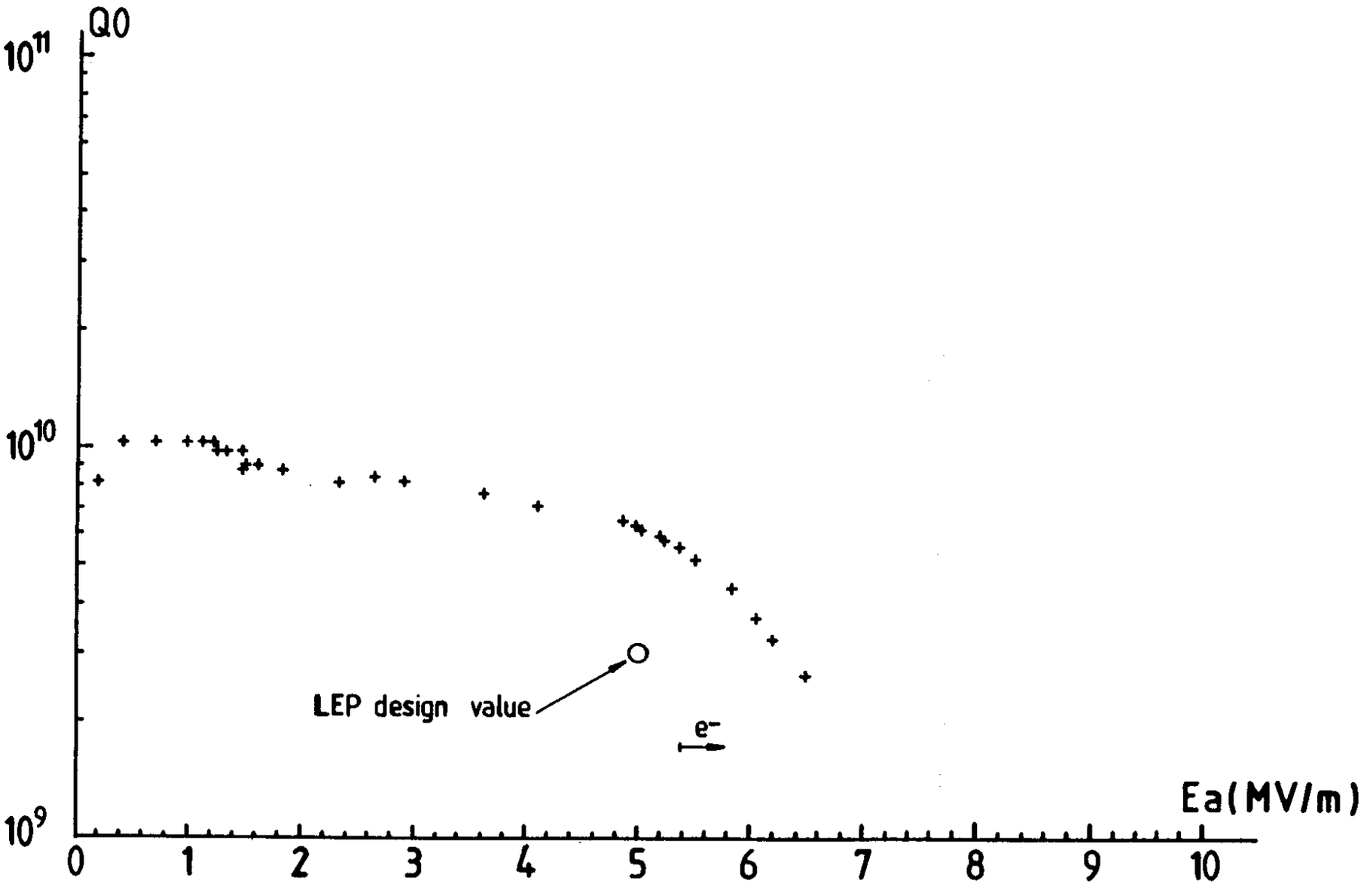

Figure 13